Assessment of the Wake-Vortex Encounter Probability on Final Approach based on Lidar Measurements

Stephan Körner*, Frank Holzäpfel†

Deutsches Zentrum für Luft- und Raumfahrt, Institut für Physik der Atmosphäre, Oberpfaffenhofen, Germany

This paper assesses possible wake vortex encounters in lidar field measurements accomplished by DLR and NASA at major international airports (Munich, Frankfurt, Dallas, Denver, Memphis) comprising 8820 aircraft landings. Therefore, the applied separations are analyzed depending on the aircraft pairings and compared to the ICAO and RECAT standards. Further, we evaluate the distances between the wake generated by the leading aircraft and the follower. The results reveal that in 3.6% of the landings with an initial altitude under 50 m the luff vortex remains within a distance of 50 m to the follower within a temporal buffer of ± 10 s of flyby. In only 0.02% of the landings the encounters exceed a roll-control ratio of 0.2, a limit beneath which encounters are considered acceptable by pilots.

*Research Scientist, Institute of Atmospheric Physics, DLR, Oberpfaffenhofen, Germany.
†Senior Research Scientist, Institute of Atmospheric Physics, DLR, Oberpfaffenhofen, Germany.

Nomenclature

a/c	aircraft
b	vortex spacing
$C_{l,wv}$	normalized rolling momentum induced by vortex
$C_{l,a/c}$	maximum rolling momentum of aircraft with full rudder deflection
N	Brunt Väisälä frequency
RCR	Roll-Control Ratio
r_d	radial distance between wake of leader and track of following aircraft
t	time
t_b	buffer between lidar time stamp and time of flyby of follower
u	axial velocity component
$u_{a/c}$	ground speed aircraft
w	vertical velocity component
y	lateral vortex position
z	vertical vortex position

Greek

Γ	vortex strength in terms of circulation
σ	standard deviation

Subscript

n	number of observations
0	initial value

Superscript

$*$	normalized quantity

I. Introduction

Wake vortices [1], generated at the wings of aircraft as a response to lift, can induce a potentially hazardous rolling moment to any follower. This can lead to dangerous situations, especially in the terminal area, where pilots may not have enough time to regain control over the aircraft at low altitudes. To prevent accidents ICAO elaborated separation standards [2, 3] for specified aircraft pairings that are currently under revision [4, 5]. Nevertheless, these measures cannot fully evade wake encounters in airport vicinity. Data collected by the United Kingdom Civil Aviation Authority between the years 1982 and 1990 [6] contains 1089 incidents of which the vast majority occurred at London Heathrow. In half of the cases the required minimum separation was deceeded. An evaluation of the Aviation Safety Reporting System (ASRS) database by Münster and Schwarz [7] lists 488 reported wake encounters and 58 incidents (physical or personal damage) between the years 1999 and 2009 of which most occurred during approach and landing. Most of the encountering aircraft were medium-sized (75.8%) behind a medium (53%) or heavy aircraft (41.3%). More recently, the ASRS database lists 277 encounters reported by pilots between 01/2016 and 01/2018 in the USA.

Despite the availability of these pilot reports, the real number of wake vortex incidents is, however, hard to estimate, as reports are not mandatory and even if they are filed there is no way to tell whether the reported incident can indeed be ascribed to wake turbulence or atmospheric turbulence. Also, there is discrepancy between what pilots report and what the flight recorders capture. As a consequence there is a lack of reliable and published statistical data about the number and severity of wake vortex incidents in the glide slope. Instead, various studies were performed to estimate the encounter frequency based on models. Holzäpfel et al. [9] developed the WakeScene package that utilizes a model traffic mix, aircraft trajectories, meteorological conditions, wake-vortex evolution, and potential hazard areas to assess the encounter probabilities for crosswind departures employing Monte Carlo simulations in a domain ranging from the runway to an altitude of 3000 ft above ground. A simulation with a sample size of 100.000 approaches of heavy aircraft with medium-sized followers [9] confirmed that most encounters occur below an altitude of 300 ft above ground [10], while the strongest encounters were found at higher altitudes.

Schumann et al. simulated the number of encounters en-route based on a linear model over North America in 46 days for radar-observed traffic [11] and found that encounters typically occur at a horizontal separation of 20-30 km and often for similar flight directions. They state that with 26% the largest fraction of these encounters occurs when both aircraft are descending. Further, unpublished long-term lidar measurements of wake vortices at Charles de Gaulle airport suggest that in 3% of the cases, the vortices are at least as close as 25 m in radial distance to following landing aircraft in proximity of the threshold [12].

In recent years DLR and NASA have collected a respectable amount of lidar wake vortex field measurements at major international airports themselves with the goal to better understand wake vortex behavior at different generation altitudes under various meteorological conditions and to train their fast-time models [13, 14, 15, 16, 17, 18, 19]. The DLR campaigns comprise measurements from Munich (WakeMUC) [20] and Frankfurt (WakeFRA) [21], while the NASA dataset has been accomplished at the airports of Memphis (MEM95, MEM13) [22, 23], Denver (DEN03) [24] and Dallas (DFW97) [25]. All measurements comprise the vortex position, circulation and age as well as the time stamp of the aircraft when passing the lidar measurement plane that is oriented perpendicular to the flight direction.

In this study we analyze to which extent the applied separations conform with the ICAO and RECAT standards by utilizing the lidar time stamps and the aircraft types. Further, we estimate the temporal buffer and distance between the vortices

generated by a leading aircraft and the follower to assess the number of potential wake encounters in the glide slope. With this information we can conclude how the aircraft reacts on average during an encounter. Instead of normalizing the wake vortex parameters as usually, we employ dimensional data in this study. As vortex transport due to crosswind is crucial for this analysis the vortices are categorized into luff and lee according to the lateral drift observed in the first 9 measurements for each landing. To evaluate the severity of the potential encounters the roll-control-ratio is applied.

A. Measurements

The measurements of the employed field campaigns differ in vortex generation height, traffic mix, meteorological conditions and also in their quality. In order to produce robust results only landings are employed that satisfy a certain quality standard. Landings where either the luff or lee vortex measurement does not meet the criteria $|\Gamma^*_{0,\mathrm{lidar}} - \Gamma^*_{0,a/c}| < 0.5$, indicating poor quality measurements, are excluded from the NASA datasets. Γ^* here stands for the normalized circulation, derived by Γ/Γ_0. For the WakeMUC dataset the cases have been handpicked. From the WakeFRA campaign only landings on runway 25R are utilized, although landings from 25L are also available, however with nonuniform signal to noise ratios [19]. Further note, that in the WakeFRA campaign only the landings of heavy aircraft were captured such that in many cases the follower might not be available in the measurements. Due to the naturally large separations during off-peak the concerned cases could not be identified. The number of total and quality checked landings distributes as listed in Table 1.

Table 1: Number of total and quality checked landings.

campaign	total	quality checked
DFW97	208	190
MEM95	305	277
DEN03	772	764
WakeFRA	290	162
WakeMUC	907	374
MEM13	8183	7053

An overview of the vortex generation heights z_0 and the approach velocity of the aircraft at the time of flyby is depicted in Fig. 1. Most vortices have been generated below 120 m such that the interaction with the ground plays a significant role. As the vortex pair descends as a result of mutual velocity induction it approaches the ground and sheds off secondary vorticity [1, 19]. The latter induces the vortices an upwards directed velocity, causing them to rebound [1, 19].

The approach velocity in the WakeMUC measurements is not given for which reason it is assumed to be 70 m/s. For the other campaigns the median aircraft velocity amounts to 71.8 m/s, with the approach at Denver airport being slower than at the other airports. Further, the aircraft type in the WakeMUC dataset is unknown, which is why the aircraft weight is calculated from the measured initial vortex circulation. In all other campaigns the weight and b_0 can be determined from the aircraft types.

B. Uncertainties

The employed wake vortex measurements are associated with uncertainties with respect to the limited lidar resolution, processing of the lidar derived velocity spectra to compute vortex position and circulation, lidar time stamp and finally aircraft initial conditions. According to a study by Köpp et al., who compared the 2-μm pulsed Doppler lidar of DLR and the 10-μm continuous wave Doppler lidars from ONERA and QinetiQ, the standard deviations were $\sigma_{\mathrm{err},z} = 9$ m, $\sigma_{\mathrm{err},y} = 12$ m and $\sigma_{\mathrm{err},\Gamma} = 13$ m^2/s. The uncertainties about the aircraft initial conditions and the lidar time stamps remain unknown. The relative aircraft position is wherever available derived from the GPS signal and lidar position. Otherwise the position is computed from the first lidar measurement. Further uncertainty is imposed by the missing capability of the lidar algorithm to track vortices after they have decayed to a certain extent due to their declining coherency. Our measurements show that most vortices with a circulation less than $0.5\Gamma_0$ cannot be tracked anymore. Therefore, this study can only reveal encounters with still coherent vortices, while many encounters with less coherent vortices may remain undetected.

II. Applied Separation

Fig. 2 depicts both the temporal and spatial separation of the aircraft pairings in the dataset. The temporal separations in all campaigns are very much alike with the exception of WakeFRA. Frankfurt features two parallel runways that cannot fully be used independently. However, we only employed landings from 25R which explains this deviation from the other campaigns. Most pairings exhibit a separation of about 110 s. The spatial separations distribute very similar as the temporal with regard to their shape. Here, the maximum lies at 4 nautical miles, with exception of WakeFRA where most pairings feature a separation of 8 nautical miles.

With the aircraft types of the leading and following aircraft the required separation can be derived from a look-up table. In a next step this can be compared to the applied separation between the two aircraft. The results are illustrated in Fig.

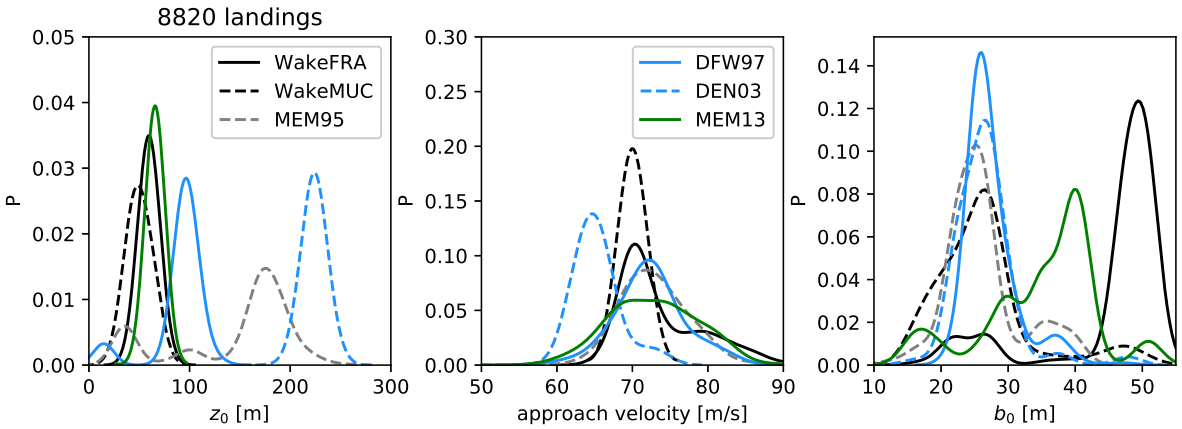

Fig. 1: Distribution of vortex generation height and approach velocity.

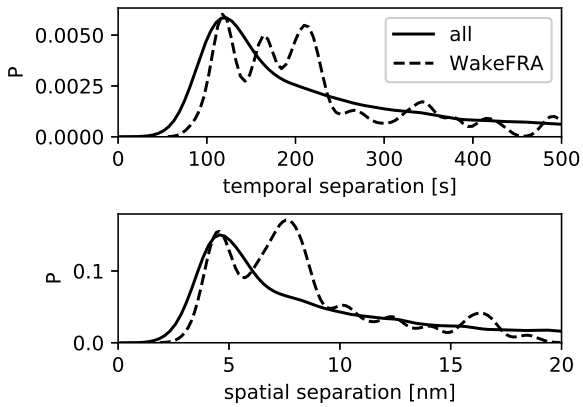

Fig. 2: Temporal and spatial separation between the aircraft.

3. The left column depicts the number of landings against the applied separation, clustered into the separations that should have been applied following the ICAO or RECAT rules [2, 3, 5, 26]. As Memphis airport already applied the RECAT separation during the latest field measurements the MEM13 campaign is analyzed separately. We assume that radar separation always amounts to 2.5 nm which can only be applied under favorable conditions. Otherwise, it amounts to 3 nm such that our evaluation is conservative concerning critical separation discrepancy. While the vast majority of the pairings fell under an ICAO separation of 2.5 nm for the MEM95, DFW97, DEN06, WakeFRA and WakeMUC campaigns, most separations in the MEM13 field campaign were assigned to 3 nm according to RECAT.

The discrepancy between required and applied separation is illustrated in the right column of Fig. 3 - both if ICAO and RECAT standards were applied. Negative values denote under-separation. These results suggest, that under-separation occurs in 2.6% of the landings in the MEM95, DFW97, DEN06, WakeFRA and WakeMUC campaigns. In 0.3% of the landings the under-separation exceeds 1 nm. These cases can mainly be assigned to the landings where 5 nm ICAO separations should have been applied. It is interesting that the difference between ICAO and RECAT rules is negligible for the analyzed traffic mix. In the MEM13 dataset in only 0.8% of the landings under-separation occurs and in 0.06% of the pairings an under-separation of 1 nm is exceeded under the applicable RECAT rules. Here, the difference to the ICAO rules is much larger as RECAT allows a smaller separation to the leader for the very frequently DC10 and MD11 aircraft of FedEx that approach Memphis airport.

Note, that this illustration only shows the temporal overlap between the follower and the wake of the leading aircraft but not the distance to the wake. Even if there is a temporal overlap of 50 s the wake can already be distant enough to pose no danger.

III. Identification of Possible Wake Vortex Encounters

To identify an encounter in our dataset the time stamp of the lidar measurement must be within a specified time interval centered at the time of flyby of the follower and its position must be close enough to the the measured vortex core.

A. Temporal buffer

In a first step we evaluate the temporal buffer between each last measured vortex of a recorded wake track and the time of flyby of the follower. Fig. 4 illustrates the distribution of these buffers, with negative values denoting an overlap. Temporal overlaps can especially be found in the MEM13 and DEN03 campaigns. This can be referred to the fact that the NASA lidar algorithm is capable of identifying 4 wake vortices at a time, given their separation is not too small. In contrast, vortices in the DLR dataset are usually only tracked until the fol-

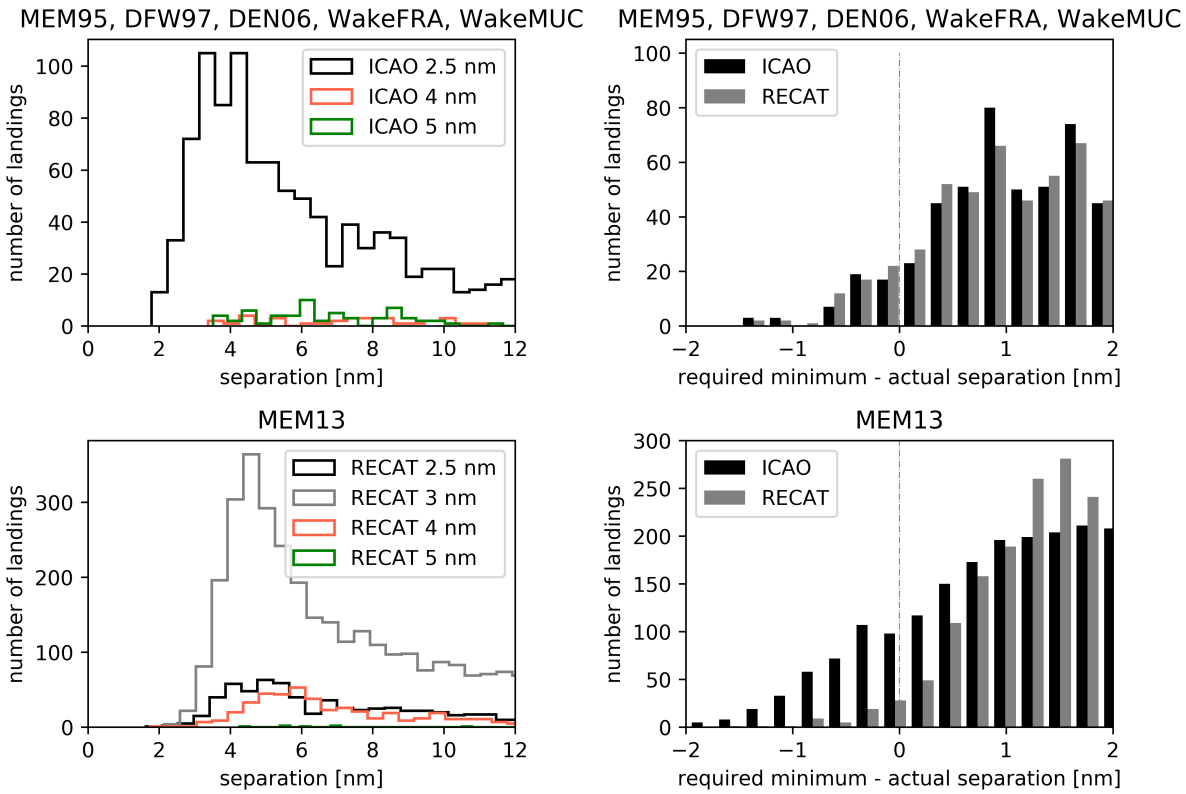

Fig. 3: Applied separation clustered according to the applicable ICAO and RECAT standards.

lowing aircraft passes the measurement plane, with the exception of a few manually processed landings. Therefore, the interest does not solely lie upon buffers below but mainly upon buffers just around zero. Vortices with a temporal buffer below zero that were obviously tracked incorrectly are neglected.

The probability that the luff vortex can still be detected 20 s before the follower arrives amounts to 11.5% on average in our dataset. It reduces to 7.1% for 10 s and to 2.4% for a buffer of 0 s. Due to the interaction with the ground the lee vortex usually is shorter-lived than the luff vortex [19]. Consequently we would expect the buffers of the lee vortex to be larger. This trend is, however, only pronounced in the WakeMUC dataset. Therefore, similar probabilities are observed for the lee vortices.

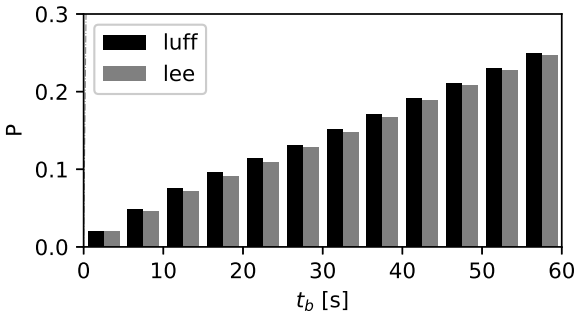

Fig. 4: Cumulative distribution of the temporal buffer between the last measured wake generated by the leader and time of flyby of the follower through the measurement plane for the luff and lee vortex.

B. Spatio-temporal buffer

Note, that this does not yet give any indication on the number of encounters, as the distance between the wake and the follower has been neglected so far. By comparing the time and position of the individual lidar measurements with the time the of flyby and position of the following aircraft we can calculate the distance of the wake from the flight path. Fig. 5 depicts the lateral distance of all measured vortices relative to the flight track of the follower. Negative y-values indicate the luff and positive y-values the lee direction. Green and red measurements denote vortices that have been tracked within a time interval of ± 10 s relative to the flyby of the follower. This analysis illustrates that the lee vortex is usually transported out of the glide slope, whereas a considerable part of the luff vortex measurements overlap with the track of the follower. This is also the case for the vortices in temporal proximity to the flyby of the follower, rendering an encounter with the luff vortex potentially more likely than with the lee vortex (see also

[19]). The fact that some of the lee vortex measurements can be found on the luff side can be owed to the crosswind being variable, especially under low-wind conditions, such that the categorization of the vortices into luff and lee based on the drift of the first measurements may be flawed at later times.

Furthermore, the results indicate that some of the vortices that can still be tracked within the buffer of ± 10 s are located within a lateral distance of less than 50 m. Although in the majority of the cases the vortices have already reached an age of above 60 s vortex strengths of above 300 m^2/s can be found. Nevertheless, the results also underpin that a large part of the vortices is advected and poses no danger to the follower.

To further limit the number of possible encounters Fig. 6 illustrates the vertical against the lateral vortex position relative to the position of the following aircraft. Again, a time interval of ± 10 s is applied to detect vortices in temporal proximity of the follower flyby (red and green symbols). Note, that the underlying dataset comprises various vortex generation altitudes which are connected with different vortex behavior. For this reason the plot features a transition at about -50 m that is caused by the ground in the measurements with low vortex generation altitudes.

Due to their property to descend most of the vortices are located below the position of the follower, especially when generated at high altitudes. In ground proximity, however, the vortices may rebound and even rise above their generation altitude. It is remarkable that in the plots nearly all vortices that can still be tracked at the time of flyby are located below the follower, although the dataset contains a large amount of landings with vortex generation altitudes below $2b_0$ where rebound is expected.

A statistical analysis of wake distance from the following aircraft for various buffers t_b is depicted in Fig. 7. As already inferred from Fig. 6, the number of measured luff vortices being close to the track of the follower exceeds the respective number for the lee vortex. In the interval $0 < t_b < 20$ s the luff vortex of the leading aircraft still persisted in a radial distance of below 50 m (25 m) to the follower in 348 (48) measurements. For the interval $-10 < t_b < 10$ s this number still amounts to 153 (31).

Fig. 8 shows this statistics in terms of landings rather than in terms of measurements for the time buffer interval of $-10 < t_b < 10$ s. At 138 (25) landings the luff vortex of the leader has been detected in a radial distance below 50 m (25 m) of the follower. This number corresponds to 1.6% (0.3%) of all analyzed landings (8820). For the lee vortex these numbers are with 35 (2) landings, corresponding to 0.4% (0.02%), substantially smaller. We find that the initial altitudes of the aircraft in this subset were all below 90 m, which can be accounted to the less pronounced rebound of the vortices if generated above this altitude. Fig. 9 illustrates that the probability of an encounter with the luff vortex increases for decreasing initial altitudes and decreases to zero below an altitude of 50 m, where the rebound of the luff vortex is suppressed for increasing crosswind speeds [19] and where vortex decay is further enhanced due to vortex-ground interaction and end-effects [27, 28]. Including only measurements with $z_0 < 90$ m, the probability to detect the luff vortex within 50 m (25 m) radial distance of the follower increases to 1.8% (0.3%). For landings with z_0 below 50 m this number further increases to 3.6% (1.5%). In contrast, the probability to encounter the lee vortex decreases with lower altitudes, which can be referred to the stronger interaction with the ground for lower generated vortices that leads to an increased divergence of the vortex pair. The increased encounter probability between 50 m and 60 m altitude confirms that the height ranges utilized for safety cases for example for RECAT EU are reasonable.

Compared to Holzäpfel et al. [9] our values are significantly lower. They find that the frequency to encounter a vortex below 300 ft within a distance of 30 m with a circulation of at least 200 m^2/s (100 m^2/s) amounts to 6% (4%). These numbers correspond to 0.12% (0.40%) in our study for a temporal overlap of ±10 s.

IV. Encounter Severity

A. Roll-Control Ratio

In order to correctly classify the detected encounters the severity of the incident must be assessed. An often applied severity measure is the Roll-Control Ratio (RCR) [29]. It is the ratio of the rolling momentum $C_{l,wv}$ that is imposed on the aircraft and the maximum rolling momentum $C_{l,a/c}$ that it can achieve with full rudder deflections.

$$RCR = \frac{C_{l,wv}}{C_{l,a/c}} \tag{1}$$

We assume $C_{l,a/c} = -0.1$ which is an average over various aircraft types based on Schwarz and Hahn [30]. Schwarz and Hahn [29] concluded from flight simulator tests that pilots rated wake encounters with RCRs below 0.2 as acceptable. Nevertheless, in their simplified hazard area prediction (SHAPe) model they also include RCRs of 0.1 as hazard areas.

The induced rolling momentum $C_{l,wv}$ is computed according to Hennemann [31] based on the vertical velocity component w, axial velocity component u and aircraft speed $u_{a/c}$. $C_{l,wv}$ is normalized by dividing by dynamic pressure, wing area and half wing span [31], which leads to Eqn. (2). Note, that this is a German convention and that the full wing span is employed for normalization in

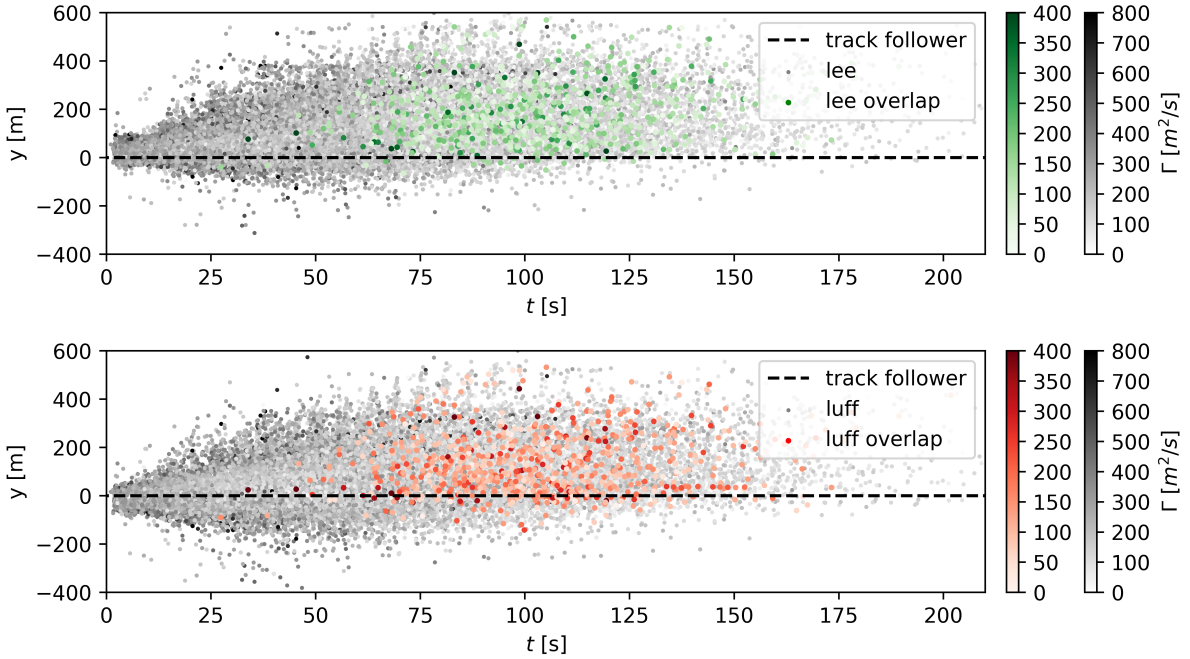

Fig. 5: Lateral position of the vortices (all measurements) relative to the position of the following a/c. The circulation is color-coded. Red and green vortices denote a temporal overlap of ± 10 s of the measurement relative to the time the follower passes.

the USA.

$$C_{l,wv} = \frac{8}{B^2} \int_{-B/2}^{B/2} \sqrt{1 - \left(\frac{y}{B/2}\right)^2} \cdot \arctan\left(\frac{w(y)}{u(y) + u_{a/c}}\right) y \, dy \tag{2}$$

We assume that the encountering aircraft flies parallel to the vortex such that the axial velocity component equals 0. Further, we set the vortex core radius r_c to 3.5% of the wing span as suggested by Schwarz and Hahn [29]. The velocity fields of the vortex pairs are derived from the Burnham-Hallock vortex model [32], taking into account the measured vortex circulation. To model the effect of the ground image vortices [33] are introduced.

B. Results

The RCR is computed for all landings where the following aircraft passed the measurement plane in a time interval of ± 10 s of a valid vortex measurement. For each landing only the measurement with the smallest time difference to the flyby is picked. The flow field is discretized with a spatial resolution of $dy = dz = 1$ m. If both the measurements of the luff and lee vortices are available the velocity field is computed based on the vortex pair. Otherwise only a single vortex is employed to derive the velocity field. The resulting RCRs together with the vortex positions are plotted in Fig. 10. We find that the maximum RCR in the analyzed dataset amounts to $|RCR| = 0.22$ and is thus above the value of 0.2 below which encounters have been rated acceptable by pilots [29]. In that case a B777 aircraft (heavy according to ICAO or upper heavy according to RECAT) encounters the vortex pair with a remaining circulation of 350 m^2/s of a leading aircraft of the same type. This encounter situation is displayed in Fig. 11 and shows the follower just above the luff vortex. The vortex was measured 5.8 s before the flyby of the leading aircraft. During the encounter the follower does not only experience a rolling-momentum but also, additional to the crosswind, a weak vortex-induced sidewind component of 0.1 m/s (at the center of the fuselage) and a downdraft of 1.8 m/s (averaged over the wingspan).

The second most severe encounter involves a MD11 (heavy according to ICAO or lower heavy according to RECAT) entering the luff vortex of a leading MD11 (see 12). Although the vortices only have a remaining circulation of 189 m^2/s (luff) and 240 m^2/s (lee) the $|RCR|$ amounts to 0.20 as a result of the small distance to the vortex core and the small vortex separation. In the MEM13 campaign low divergence can often be observed. We suppose that this is related to the interaction of the vortices with the forest canopy as discussed in Delisi et al. [34]. The aircraft further experiences an additional sidewind component of 1.6 m/s and a downdraft of 2.0 m/s, transporting it eventually downward into a region with even higher rolling momentum.

In both cases the vortices first descend and then rebound up to flight altitude before being encountered by the follower. As a result of the interac-

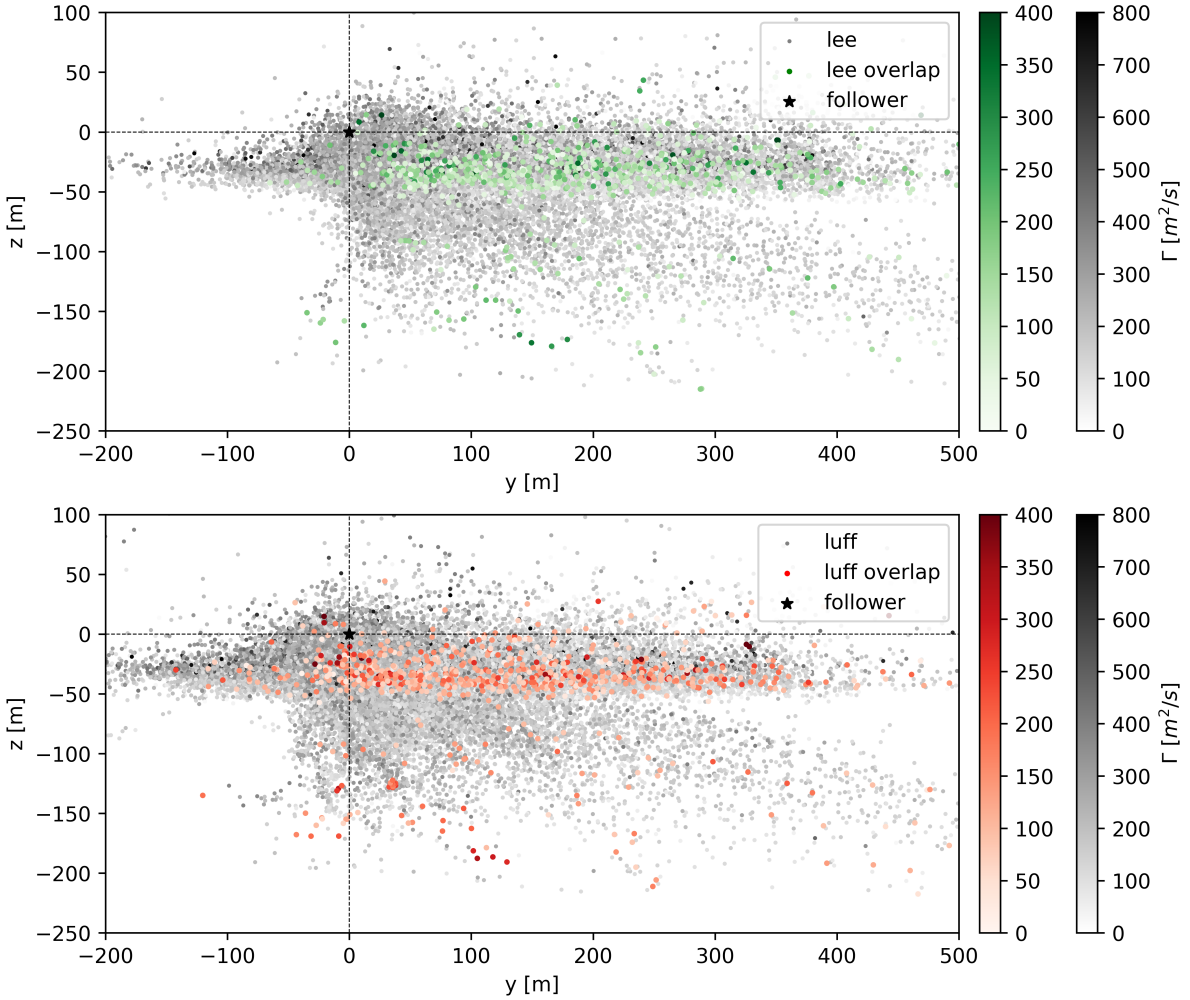

Fig. 6: Position of the vortices (all measurements) relative to the position of the following a/c. The circulation is color-coded. Red and green vortices denote a temporal overlap of ± 10 s of the measurement relative to the time the follower passes.

tion with the ground the vortex spacing would be expected larger after rebound. However, in the discussed cases this is only observed for the B752 landing.

Overall, the RCR exceeds 0.2 (0.1) at 7 (13) landings which corresponds to 0.13% (0.24%) of all aircraft pairings. If only landings for $z_0 < 90$ m are evaluated the percentage increases to 0.13% (0.26%). For $z_0 < 50$ m the RCR never exceeds 0.1 and is only at 2 landings above 0.1 (0.55%). For some measurements relatively large RCRs are identified in a lateral distance of 40 m or more of the aircraft. This is either due to the other vortex of the pair being closer to the following aircraft or due to the relatively small size of the follower combined with high remaining circulation of the vortices. Keep in mind, that in some cases the luff and lee direction could not be assigned to the vortices correctly due to varying wind conditions.

V. Conclusion

This paper analyzes a dataset that contains lidar measurements of the wake vortices generated by 5431 aircraft during final approach to assess the probability of wake vortex encounters during this phase. The measurements have been accomplished by NASA at the airports of Memphis, Denver and Dallas and by DLR at Frankfurt and Munich airport. Beside the position, circulation and age of the vortices the measurements also contain the time of flyby and the type of the vortex-generating and following aircraft. In a first step we utilize this information to compute the applied separation and compare it with the required separation according to ICAO and RECAT. In the campaigns where ICAO separation is applied under-separation occurs in 2.6% of the landings. Large non-conservative deviations from the rules mostly occur for a separation of 5 nm. The newest Memphis campaign exhibits under-separation in only 0.8% of the landings (RECAT separation).

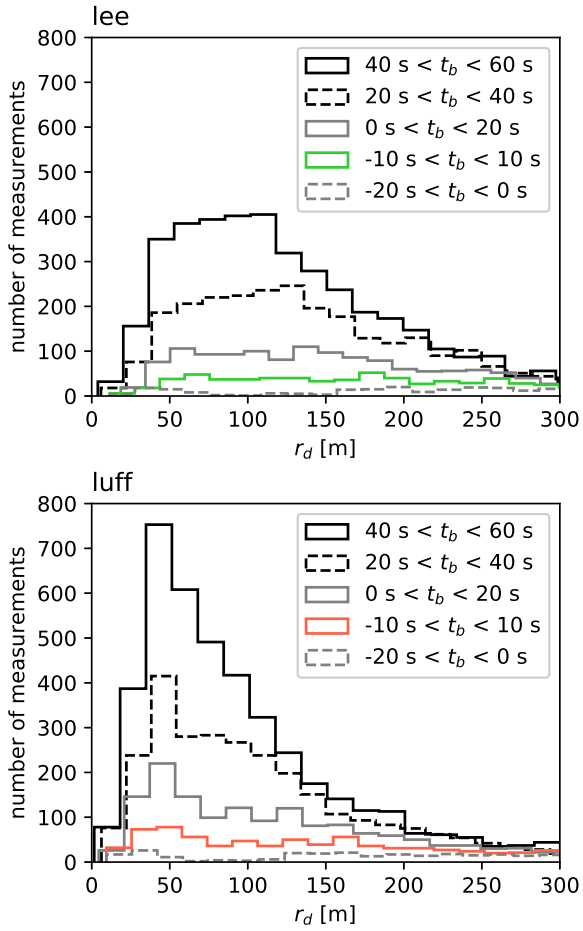

Fig. 7: Distribution of the radial distance between the follower and the measured wake vortex positions of the leader for the luff and lee vortex.

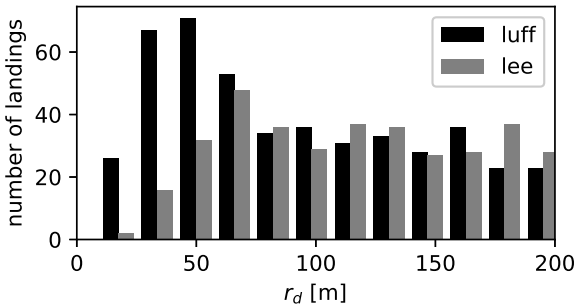

Fig. 8: Distribution of the radial distance between the follower and the temporal closest wake of the leader for each landing for the luff and lee vortex for a temporal buffer of ±10 s.

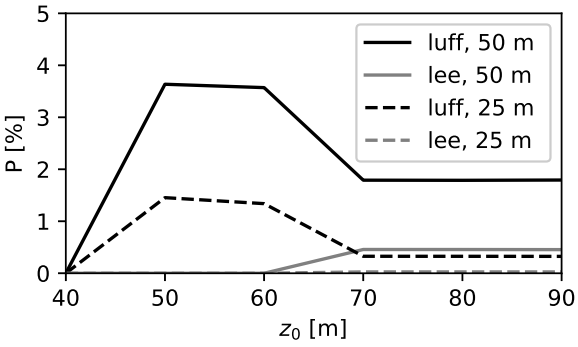

Fig. 9: Percentage of vortices within a radial distance of 50 m or 25 m of the following aircraft for a temporal buffer of ±10 s for a given z_0 of the leader or below.

In 7.1% of the landings the wake vortices of the leading aircraft can still be sensed 10 s or less before the follower arrives. Further, we find that that the luff vortex has been detected in a radial distance below 50 m (25 m) of the follower in 1.6% (0.3%) of the landings within a temporal buffer of ±10 s. If only landings with initial altitudes below 50 m are evaluated, where encounters are more likely due to the vortex rebound, this number increases to 3.6% (1.5%). Due to the lateral transport, caused by the vortex ground-interaction overlaid by crosswind, the probability to encounter the lee vortex is considerably smaller. We also find that the probability of an encounter with the luff vortex increases with decreasing altitude and decreases again slightly below an altitude of 50 m. Note, that our numbers are below the 3% found by Treve. However, we neither know the exact altitude interval of their measurements nor the quality of their data.

In the identified cases where an encounter might have occurred most vortices are located below the following aircraft, which can partly be attributed to the z_0 distribution in our dataset and the rebound of the vortices being limited. However, even in the cases where the vortices are generated in ground proximity the rebound rarely exceeds the initial altitude z_0.

To assess the encounter severity of the cases where the vortices were in proximity of the following aircraft the roll-control ratio [29, 35] is computed. This measure is derived from the remaining vortex circulation, its relative position to the follower and the specifications of the following aircraft. It specifies the ability of the follower to counteract the rolling-momentum imposed by the vortex. We find that a value of 0.2, below which pilots rated wake encounters as acceptable, is exceeded at 2 landings which corresponds to 0.02% of the approaches in this dataset. A roll-control ratio of 0.1 is exceeded at 13 landings (0.24%). This demonstrates that although many vortices still hover in the vicinity of the glide path, severe encounters occur rarely in the analyzed dataset. This can be referred to the characteristics of the vortices to be advected by the wind and to descend. Only if they rebound up to flight altitude at low crosswind speed, that compensates the divergence they experience in

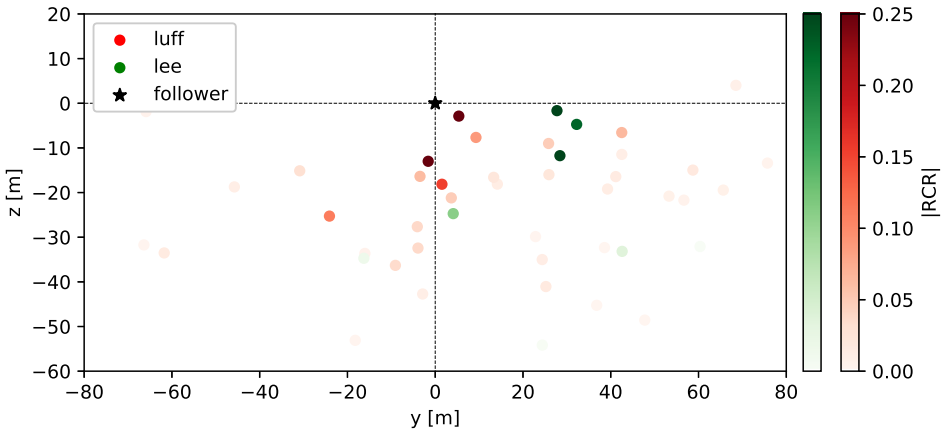

Fig. 10: Absolute roll-control ratio for vortex measurements with a temporal overlap of ± 10 s relative to the time the follower passes. For each landing only the measurement with the smallest time difference to the flyby is picked.

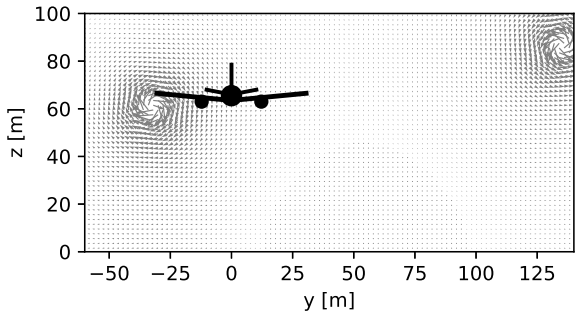

Fig. 11: Most severe encounter ($RCR = 0.22$) in the dataset of a Boeing 777 in the wake of an aircraft of the same type.

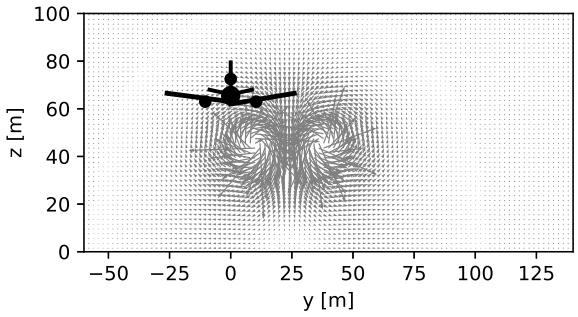

Fig. 12: Second most severe encounter ($RCR = 0.20$) in the dataset of a MD11 in the wake of a leading aircraft of the same type.

ground proximity, a severe encounter can occur.

However, the probability of a vortex encounter increases with decreasing initial altitude z_0. A further study that features a larger amount of landings captured below 50 m would thus be very valuable.

Acknowledgments

We thank Nash'at Ahmad from the NASA Langley Research Center for his continuous support and the provision of the NASA wake vortex field measurement data.

References

[1] Hallock, J. N. and Holzäpfel, F., "A review of recent wake vortex research for increasing airport capacity," *Progress in Aerospace Sciences*, 2018.

[2] ICAO, J., "Rules of the Air," *Annex 2 to the Convention on International Civil Aviation, Chicago, IL*, Vol. 10, 2005.

[3] Rooseleer, F. and Treve, V., "European Wake Turbulence Categorisation and Separation Minima on Approach and Departure," report 1.1, Eurocontrol, 2015.

[4] Doe, R., "Caution Wake Turbulence: New Rules for the EU," April 2016, http://flightservicebureau.org/caution-wake-turbulence-new-rules-for-the-eu/.

[5] "Implementation of the RECAT-EU Wake Turbulence Separation Scheme at Paris Charles De Gaulle, Paris-Le Bourget and Pointoise-Cormeilles-En-Vexin airports from March 22nd 2016," report A 03/16, Direction des Opérations, Service de l'Information Aéronautique, 2016.

[6] J.B. Critchley, P. F., "UNITED KINGDOM CIVIL AVIATION AUTHORITY WAKE VORTEX DATABASE: ANALYSIS OF INCIDENTS REPORTED BETWEEN 1982 AND 1990," report CAA PAPER 91015, CIVIL AVIATION AUTHORITY LONDON, 1991.

[7] Münster, C. and Schwarz, C., "Auswertung von Wirbelschleppenmeldungen im US Aviation Safety Reporting System (ASRS)," report IB 111-2010/33, Deutsches Zentrum für Luft- und Raumfahrt, 2010.

[8] "ASRS Database Report Set, Wake Turbulence Encounters," report 262-7, NASA, 2017.

[9] Holzäpfel, F., Frech, M., Gerz, T., Tafferner, A., Hahn, K.-U., Schwarz, C., Joos, H.-D., Korn, B., Lenz, H., Luckner, R., et al., "Aircraft wake vortex scenarios simulation package – WakeScene," *Aerospace Science and Technology*, Vol. 13, No. 1, 2009, pp. 1–11.

[10] Claire Pugh, Antoine Vidal, H. H., "Aircraft Wake-Vortex Evolution in Ground Proximity: Analysis and Parameterization," *Wake Vortex Research Needs for improved wake vortex separation ruling and reduced wake signatures*, Vol. 2, 2006, pp. 68–74.

[11] Schumann, U. and Sharman, R., "Aircraft wake-

vortex encounter analysis for upper levels," *Journal of Aircraft*, Vol. 52, No. 4, 2014, pp. 1277–1285.

[12] Treve, V., "Research needs for operational concepts and capacity analysis," Discussions during WakeNet3- Europe Workshop, London, 2011.

[13] Sarpkaya, T. et al., "Wake-Vortex Eddy-Dissipation Model Predictions Compared with Observations," *Journal of Aircraft*, Vol. 38, 2001, pp. 687–692.

[14] Robins, R. E., Delisi, D. P., and Greene, G. C., "Algorithm for Prediction of Trailing Vortex Evolution," *Journal Aircraft*, Vol. 38, No. 5, 2001.

[15] Robins, R. E. and Delisi, D. P., "NWRA AVOSS Wake Vortex Prediction Algorithm Version 3.1.1," research report NASA/CR-2002-211746, Northwest Research Associates, Inc., Bellevue, Washington, USA, 2002.

[16] Holzäpfel, F., "Probabilistic Two-Phase Aircraft Wake-Vortex Decay and Transport Model," *Journal of Aircraft*, Vol. 40, 2003, pp. 323–331.

[17] Holzäpfel, F., "Probabilistic Two-Phase Aircraft Wake-Vortex Model: Further Development and Assessment," *AIAA Journal*, Vol. 43, No.3, 2006, pp. 700–708.

[18] Proctor, F. H., Hamilton, D. W., and Switzer, G. F., "TASS driven algorithms for wake prediction," *44th AIAA Aerospace Sciences Meeting and Exhibit, AIAA*, , No. 2006-1073, 2006.

[19] Holzäpfel, F. and Steen, M., "Aircraft Wake-Vortex Evolution in Ground Proximity: Analysis and Parameterization," *AIAA Journal*, Vol. 45, 2007, pp. 218–227.

[20] Holzäpfel, F., Tchipev, N., and Stephan, A., "Wind impact on single vortices and counterrotating vortex pairs in ground proximity," *Flow, Turbulence and Combustion*, 2016, pp. 1–20.

[21] Frech, M. and Holzäpfel, F., "Skill of an Aircraft Wake-Vortex Model using Weather Prediction and Observation," *Journal of Aircraft*, Vol. 45, 2008, pp. 461–470.

[22] S.D.Campbell, T.J.Dasey, R.E.Freehart, R.M.Heinrichs, M.P.Matthewsa, G.H.Perras, and G.S.Rowe, "Wake Vortex Field Measurement Program at Memphis, TN Data Guide," research report NASA/L-2. 1997, Lincoln Laboratory, Massachusetts Institute of Technology, 1997.

[23] Pruis, M. J., Delisi, D. P., Jacob, D., and Lai, D., "Summary of NASA Wake and Weather Data Collection at Memphis International Airport: 2013-2015," *8th AIAA Atmospheric and Space Environments Conference*, 2016, p. 3274.

[24] Dougherty, R. P., Wang, F. Y., Booth, E. R., Watts, M. E., Fenichel, N., and D'Errico, R. E., "Aircraft wake vortex measurements at Denver International Airport," *AIAA Paper*, Vol. 2880, No. 10, 2004.

[25] Dasey, T. J., Cole, R. E., Heinrichs, R., Matthews, M., and Perras, G., "Aircraft vortex spacing system (AVOSS) initial 1997 system deployment at Dallas/Ft. Worth (DFW) Airport," Tech. Rep. L-3, NASA/A-1, Massachusetts Inst. of Tech.; Lincoln Lab.; Lexington, MA United States, 1998.

[26] De Clercq, G. et al., "Guidelines for the application of the ECAC radar separation minima," report ASM.ET1.ST18.1000-REP-01.00, Eurocontrol, 1998.

[27] Stephan, A., Holzäpfel, F., and Misaka, T., "Aircraft wake-vortex decay in ground proximity-physical mechanisms and artificial enhancement," *Journal of Aircraft*, Vol. 50, No. 4, 2013, pp. 1250–1260.

[28] Stephan, A., Holzäpfel, F., and Misaka, T., "Hybrid simulation of wake-vortex evolution during landing on flat terrain and with plate line," *International Journal of Heat and Fluid Flow*, Vol. 49, 2014, pp. 18–27.

[29] Schwarz, C. W. and Hahn, K.-U., "Full-flight simulator study for wake vortex hazard area investigation," *Aerospace Science and Technology*, Vol. 10, No. 2, 2006, pp. 136–143.

[30] Schwarz, C. and Hahn, K.-U., "Simplified Hazard Area Prediction Method - SHAPe," Report 2011-31, Deutsches Zentrum für Luft- und Raumfahrt, 2011.

[31] Hennemann, I., "Deformation und Zerfall von Flugzeugwirbelschleppen in turbulenter und stabil geschichteter Atmospähre," Dissertation 2017-44, Deutsches Zentrum für Luft- und Raumfahrt, 2010.

[32] Nash'at, N. A., Proctor, F. H., Duparcmeur, F. M. L., and Jacob, D., "Review of Idealized Aircraft Wake Vortex Models," *52nd Aerospace Sciences Meeting, AIAA SciTech*, 2014.

[33] Corjon, A. and Poinsot, T., "Behavior of wake vortices near ground," *AIAA Journal*, Vol. 35, No. 5, 1997, pp. 849–855.

[34] Delisi, D. P., Robins, R., and Pruis, M. J., "APA3. 8 Fast-Time, Numerical Wake Model Description and Validation," *8th AIAA Atmospheric and Space Environments Conference*, 2016, p. 3437.

[35] Holzäpfel, F., Gerz, T., Frech, M., Tafferner, A., Köpp, F., Smalikho, I., Rahm, S., Hahn, K.-U., and Schwarz, C., "The wake vortex prediction and monitoring system WSVBS Part I: Design," *Air Traffic Control Quarterly*, Vol. 17, No. 4, 2009, pp. 301.